The current issue and full text archive of this journal is available at
www.emeraldinsight.com/0961-5539.htm

Numerical analysis of heat transfer enhancement in a double pipe heat exchanger with porous fins

H. Kahalerras and N. Targui
Laboratoire des Transports Polyphasiques et Milieux Poreux, Algiers, Algeria

Received 18 June 2006
Revised 16 April 2007
Accepted 25 April 2007

Abstract

Purpose – The aim is to study numerically the heat transfer enhancement in a double pipe heat exchanger by using porous fins attached at the external wall of the inner cylinder.

Design/methodology/approach – The Brinkman-Forchheimer extended Darcy model is used in the porous regions. The differential equations subjected to the boundary conditions are solved numerically using the finite volume method. Numerical calculations are performed for a wide range of Darcy number ($10^{-6} \leq Da \leq 10^{-1}$), porous fins height ($0 \leq H_p \leq 1$) and spacing ($0 \leq L_f \leq 39$) and thermal conductivity ratio ($1 \leq R_k \leq 100$). The effects of these parameters are considered in order to look for the most appropriate properties of the porous fins that allow optimal heat transfer enhancement.

Findings – The results obtained show that the insertion of porous fins may alter substantially the flow pattern depending on their permeability, height and spacing. Concerning the heat transfer effect, it is found that the use of porous fins may enhance the heat transfer in comparison to the fluid case and that the rate of improvement depends on their geometrical and thermo-physical properties. Performance analysis indicated that more net energy gain may be achieved as the thermal conductivity ratio increases especially at high Darcy numbers and heights.

Research limitations/implications – The results obtained in this work are valid for double pipe heat exchangers with the same fluid flowing at the same flow rate in the two ducts and for the case of an inner cylinder of negligible thermal resistance.

Practical implications – The results obtained in this study can be used in the design of heat exchangers.

Originality/value – This study provides an interesting method to improve heat transfer in a double pipe heat exchanger by use of porous fins.

Keywords Heat exchangers, Liquid flow, Heat transfer, Numerical analysis

Paper type Research paper

Nomenclature

C_p = specific heat at constant pressure (J/kg K)
CF = inertia coefficient, $\rho_c \varepsilon F \sqrt{K} u_{ic} / \mu_c$
D_h = hydraulic diameter, $2(r_o - r_i)$ (m)
Da = Darcy number, K/D_h^2
E = heat exchanger effectiveness
f = friction factor $(-dp_m/dx)2D_h/\rho u_m^2$
F = Forchheimer coefficient
h = convective heat transfer coefficient (W/m^2 K)
h_p = porous fins height (m)
H_p = dimensionless porous fins height, h_p/D_h
k = thermal conductivity (W/m K)
K = permeability of the porous fins (m^2)
l = heat exchanger length (m)
l_a = heat exchanger length on which are attached the porous fins (m)
l_p = porous fins width (m)
l_f = spacing between porous fins (m)

International Journal of Numerical Methods for Heat & Fluid Flow
Vol. 18 No. 5, 2008
pp. 593-617

0961-5539
DOI 10.1108/09615530810879738

L = dimensionless length of the heat exchanger, l/D_h
$\dot{m}$ = mass flow rate (kg/s)
Nu = Nusselt number, $h\,D_h/k_e$
p = pressure (Pa)
P = dimensionless pressure, $p/\rho_c\,u_{ic}^2$
Pr = Prandtl number, $\mu_c C_{pc}/k_c$
r = radial coordinate (m)
r_o = outer radius (m)
r_i = inner radius (m)
R = dimensionless radial coordinate, r/D_h
Re = Reynolds number, $u_{ic}\,\rho_c\,D_h/\mu_c$
R_k = thermal conductivity ratio, k_e/k_c
R_{kch} = thermal conductivity ratio, k_c/k_h
R_{keh} = thermal conductivity ratio, k_e/k_h
$R_{Nu\,m}$ = average Nusselt number ratio, Nu_m/Nu_{mf}
R_m = mass flow rate ratio, $\dot{m}_c/\dot{m}_h$
R_r = radius ratio, r_o/r_i
R_μ = dynamic viscosity ratio, μ_c/μ_e
$R_{\mu ch}$ = dynamic viscosity ratio, μ_c/μ_h
R_ρ = density ratio, ρ_c/ρ_h
R_α = thermal diffusivity ratio, α_c/α_h
T = temperature (K)
u = axial velocity (m/s)
U = dimensionless axial velocity, u/u_{ic}
v = radial velocity (m/s)
V = dimensionless radial velocity, v/u_{ic}
$\vec{V}$ = velocity vector
x = axial coordinate (m)
X = dimensionless axial coordinate, x/D_h

Greek symbols

ε = porosity
ρ = density (kg/m^3)
α = thermal diffusivity (m^2/s)
η = heat transfer performance ratio $(Nu_m/Nu_{mf})\cdot(f_m/f_{mf})^{-1/3}$
θ = dimensionless temperature, $(T - T_{ic})/(T_{ih} - T_{ic})$
μ = dynamic viscosity (kg/m s)
ψ = stream function

Subscripts

c = cold
e = effective
f = fluid
h = hot
i = inlet or inner
m = mean
o = exit or outer
p = porous
w = wall
x = local

Introduction

The use of solid fins to increase the heat transfer rates between two different fluids in tubular heat exchangers is one of the most effective and widely employed methods. The insertion of porous material as another technique to enhance heat transfer in these thermal systems seems to be promising. In this context, several studies have been conducted during the recent decades. Analytical solution was obtained by Chikh *et al.* (1995a) for the problem of forced convection under fully developed conditions in an annular duct partially filled with a porous layer attached to the inner cylinder on which a constant heat flux was prescribed. A similar problem, but with an isothermal boundary condition, was investigated numerically by the same authors (Chikh *et al.*, 1995b) using the Darcy-Brinkman-Forchheimer model. They showed that the porous material may be used for insulation or enhancement of heat transfer according to its physical properties. In another work, Chikh *et al.* (1997) analyzed the effect of the porous matrix addition on hydrodynamic and thermal entry lengths. The numerical study of Guo *et al.* (1997) in the annular gap of a heat exchanger showed that a significant augmentation of heat transfer and a reduction of pressure drop may be achieved by partially filling of a highly conducting porous substrate and by using pulsating flow. Bouhadef *et al.* (1999) studied the performance of an annular counter-flow heat exchanger in which a porous layer was attached to the external wall of the inner cylinder. They showed that the heat exchanger effectiveness was deeply affected by the physical properties of the porous matrix. In the same context, Alkam and Al-Nimr (1999) inserted porous substrates at both sides of the wall that separates the cold and the hot fluids. They found that the improvement in

the exchanger effectiveness is high especially at high-capacity ratios and that there is a critical value of substrate thickness beyond which there is no substantial increase in the heat exchanger performance. Pavel and Mohamad (2004) investigated numerically and experimentally the increase in the heat transfer rate when different porous media were inserted in the core of a pipe heated with a constant and uniform heat flux. They showed that heat transfer enhancement may be achieved by using porous inserts with smaller porosity and higher thermal conductivity. Allouache and Chikh (2006) presented a thermodynamic analysis in a double pipe heat exchanger with a porous layer inserted in the annular gap in order to reduce the rate of entropy generation. It was found that a porous substrate of high-effective thermal conductivity and the case of fully porous annular gap lead to a substantial reduction of the rate of entropy generation.

The use of porous fins to augment heat transfer rate is more interesting than the conventional solid ones due to their larger effective surface area and the lower pressure drop generated in comparison to the latter ones. However, their cleaning, after a long operating time, is more difficult due to the filling of the pores with dirt. Some numerical and experimental investigations have been recently performed in channels fitted with porous fins or baffles. Kiwan and Al-Nimr (2001) investigated numerically the thermal performance of porous fins attached at a hot surface and a comparison with that of conventional solid fins was conducted. It was found that more improvements in the porous fin performance may be achieved as Rayleigh number increases especially at large permeability. They also showed that there is an optimum limit for the thermal conductivity ratio beyond which there is no further enhancement in the fin performance. An experimental study was conducted by Ko and Anand (2003) in a staggered porous baffled channel in order to measure the average Nusselt number and friction factor. Experiments showed that the heat transfer enhancement per unit increase in pumping power were less than one for the range of parameters studied in this work. Yang and Hwang (2003) presented a numerical study of turbulent flow and heat transfer in rectangular channel with porous baffles mounted alternatively on the top and bottom of the walls. The k-ε model was adopted to describe the turbulent structure. It was found that the flow patterns around the porous and solid-type baffles were entirely different due to different transport phenomena and it significantly influences the heat transfer. A similar study, but for a laminar flow was conducted by Miranda and Anand (2004). The effects of dimensionless parameters such as Reynolds number, Darcy number, baffle spacing and thermal conductivity ratio on the fluid and temperature fields were examined. It was found that the average Nusselt number ratios for the solid baffles were higher than those for corresponding porous baffles.

The aim of the present numerical study is to investigate the heat transfer enhancement when porous fins are attached at the inner cylinder of a double pipe heat exchanger. This arrangement is chosen in order to increase the heat transfer surface area between the fins and the cold fluid to be heated. The effects of various parameters such as Darcy number, the height and spacing of fins and the thermal conductivity ratio on the hydrodynamic and thermal fields are analyzed.

Mathematical formulation

The physical model to be studied is a counter flow double pipe heat exchanger of length l and inner and outer radius r_i and r_o, respectively. The hot and cold fluids enter the inner cylinder and annular gap, respectively, with a uniform velocity distribution

and constant temperature. Porous fins of width l_p, height h_p and spacing l_f are attached, on a length l_a, at the external wall of the inner cylinder and the outer pipe is thermally insulated (Figure 1).

Some assumptions are made in order to simplify the problem: the flow is axisymmetric, 2D, laminar and in steady state with no internal heat generation and neglecting viscous dissipation. The thermo-physical properties of the solid matrix and the fluid are assumed to be constant and the porous medium is considered homogeneous, isotropic and saturated with a single phase fluid in local thermal equilibrium with the solid matrix. It is also assumed that the thickness of the inner cylinder of good conducting material is very weak and its thermal resistance is neglected. The length behind the last porous fin is chosen high enough so that fully developed conditions at the heat exchanger exit can be assumed.

The flow is modelled by the Brinkman-Forchheimer extended Darcy model in the porous fins to incorporate the viscous and inertia effects and by the Navier-stokes equations in the fluid domain, and the thermal field by the energy equation.

Based on the above assumptions and with the following characteristics scales:

$$X = \frac{x}{D_h}, R = \frac{r}{D_h}, U = \frac{u}{u_{ic}}, V = \frac{v}{u_{ic}}, P = \frac{p}{\rho_c u_{ic}^2}, \theta = \frac{T - T_{ic}}{T_{ih} - T_{ic}}, D_h = 2(r_o - r_i)$$

where D_h is the hydraulic diameter, u_{ic} the inlet axial velocity of the cold fluid, and T_{ic} and T_{ih} the cold and hot fluid temperature at the heat exchanger entrance, the dimensionless governing equations and their corresponding boundary conditions are given as follows:

(1) *Continuity equation:*

$$\frac{\partial U}{\partial X} + \frac{1}{R}\frac{\partial (RV)}{\partial R} = 0 \tag{1}$$

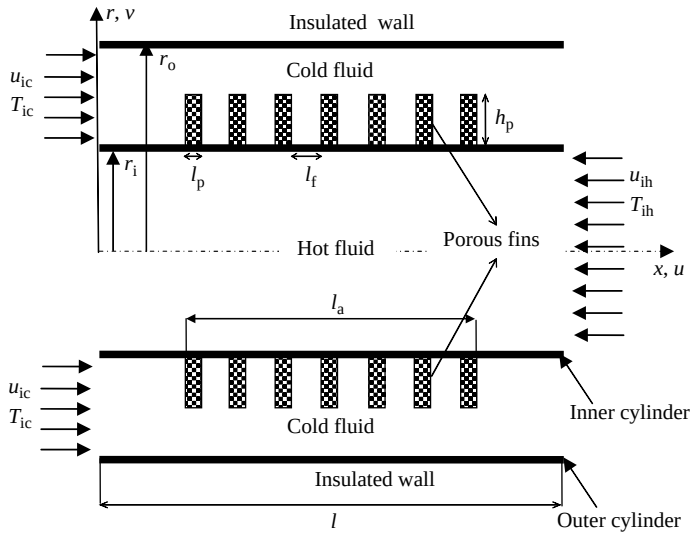

Figure 1.
Schematic of the physical domain

(2) *Momentum equations:*

- *Annular gap*:

$$\left\{\lambda\left(\frac{1}{\varepsilon^2}-1\right)+1\right\}\left[U\frac{\partial U}{\partial X}+V\frac{\partial U}{\partial R}\right]=-\frac{\partial P}{\partial X}+\frac{1}{Re}\left\{\lambda\left(\frac{1}{R_\mu}-1\right)+1\right\}\times\left[\frac{\partial^2 U}{\partial X^2}+\frac{1}{R}\frac{\partial}{\partial R}\left(R\frac{\partial U}{\partial R}\right)\right]-\frac{\lambda}{Da\,Re}U-\frac{\lambda \mathrm{CF}}{Da\,Re}|\vec{V}|U \tag{2}$$

$$\left\{\lambda\left(\frac{1}{\varepsilon^2}-1\right)+1\right\}\left[U\frac{\partial V}{\partial X}+V\frac{\partial V}{\partial R}\right]=-\frac{\partial P}{\partial R}+\frac{1}{Re}\left\{\lambda\left(\frac{1}{R_\mu}-1\right)+1\right\}\times\left[\frac{\partial^2 V}{\partial X^2}+\frac{1}{R}\frac{\partial}{\partial R}\left(R\frac{\partial V}{\partial R}\right)-\frac{V}{R^2}\right]-\frac{\lambda}{Da\,Re}V-\frac{\lambda \mathrm{CF}}{Da\,Re}|\vec{V}|V \tag{3}$$

- *Inner cylinder*:

$$U\frac{\partial U}{\partial X}+V\frac{\partial U}{\partial R}=-R_\rho\frac{\partial P}{\partial X}+\frac{1}{Re\,R_{\mu\mathrm{hc}}}\left[\frac{\partial^2 U}{\partial X^2}+\frac{1}{R}\frac{\partial}{\partial R}\left(R\frac{\partial U}{\partial R}\right)\right] \tag{4}$$

$$U\frac{\partial V}{\partial X}+V\frac{\partial V}{\partial R}=-R_\rho\frac{\partial P}{\partial R}+\frac{1}{Re\,R_{\mu\mathrm{hc}}}\left[\frac{\partial^2 V}{\partial X^2}+\frac{1}{R}\frac{\partial}{\partial R}\left(R\frac{\partial V}{\partial R}\right)-\frac{V}{R^2}\right] \tag{5}$$

(3) *Energy equation:*

- *Annular gap*:

$$U\frac{\partial \theta}{\partial X}+V\frac{\partial \theta}{\partial R}=\frac{1}{Re\,Pr}\{\lambda(R_k-1)+1\}\left[\frac{\partial^2 \theta}{\partial X^2}+\frac{1}{R}\frac{\partial}{\partial R}\left(R\frac{\partial \theta}{\partial R}\right)\right] \tag{6}$$

- *Inner cylinder*:

$$U\frac{\partial \theta}{\partial X}+V\frac{\partial \theta}{\partial R}=\frac{1}{Re\,Pr\,R_\alpha}\left[\frac{\partial^2 \theta}{\partial X^2}+\frac{1}{R}\frac{\partial}{\partial R}\left(R\frac{\partial \theta}{\partial R}\right)\right] \tag{7}$$

Where $|\vec{V}|=\sqrt{U^2+V^2}$ and λ is a binary parameter, which takes values of 0 in the fluid region and 1 in the porous region.

Boundary conditions

Owing to the elliptic nature of the governing conservation equations, the boundary conditions are specified along the entire solution domain:

- *At the inlet*:

$$X=L, 0<R<R_\mathrm{i}: U=-\frac{R_\rho\left(R_r^2-1\right)}{R_\mathrm{m}}, V=0, \theta=1 \tag{8a}$$

$$X=0, R_\mathrm{i}<R<R_\mathrm{o}: U=1, V=0, \theta=0 \tag{8b}$$

- *At the exit*:

$$X = 0, 0 < R < R_i : \frac{\partial U}{\partial X} = 0, V = 0, \quad \frac{\partial \theta}{\partial X} = 0 \tag{9a}$$

$$X = L, R_i < R < R_o : \frac{\partial U}{\partial X} = 0, V = 0, \quad \frac{\partial \theta}{\partial X} = 0 \tag{9b}$$

The length behind the last fin is chosen high enough (ten times the hydraulic diameter) to ensure that the exit boundary conditions have negligible effects on the dynamic and thermal fields:

- *At the symmetry axis*:

$$R = 0, 0 < X < L : \frac{\partial U}{\partial R} = 0, V = 0, \frac{\partial \theta}{\partial R} = 0 \tag{10}$$

- *At the inner cylinder wall*:

$$R = R_i \text{ and } 0 < X < L \begin{cases} U = 0, V = 0 \\ \left.\frac{\partial \theta}{\partial R}\right|_h = R_{k\text{ch}} \left.\frac{\partial \theta}{\partial R}\right|_c \text{(fluid} - \text{fluid)} \\ \left.\frac{\partial \theta}{\partial R}\right|_h = R_{k\text{eh}} \left.\frac{\partial \theta}{\partial R}\right|_p \text{(fluid} - \text{porous)} \end{cases} \tag{11}$$

- *At the outer cylinder wall*:

$$R = R_o, 0 < X < L : U = 0, V = 0, \frac{\partial \theta}{\partial R} = 0 \tag{12}$$

- Continuity of pressure, velocity components, stresses, temperatures and heat fluxes are invoked at porous-fluid interfaces. To ensure these conditions, the harmonic mean formulation suggested by Patankar (1980) is used to handle the abrupt changes in the thermophysical properties between clear fluid and porous media.

The dimensionless parameters appearing in the above equations are defined as:

$$Re = \frac{u_{ic}\rho_c D_h}{\mu_c}, R_\mu = \frac{\mu_c}{\mu_e}, Da = \frac{K}{D_h^2}, \text{CF} = \frac{\rho_c \varepsilon F \sqrt{K}}{\mu_c} u_{ic}, R_\rho = \frac{\rho_c}{\rho_h}, R_{\mu\text{ch}} = \frac{\mu_c}{\mu_h}$$

$$R_k = \frac{k_e}{k_c}, Pr = \frac{\mu_c C_{pc}}{k_c}, R_\alpha = \frac{\alpha_c}{\alpha_h}, R_r = \frac{r_o}{r_i}, R_m = \frac{\dot{m}_c}{\dot{m}_h}, R_{k\text{ch}} = \frac{k_c}{k_h}, R_{k\text{eh}} = \frac{k_e}{k_h}$$

Governing parameters

- *Hydrodynamic parameters.* The local friction factor in the annular gap is defined as:

$$f_x = \left(-\frac{dp_m}{dx}\right) \frac{D_h}{(\rho u_m^2)/2} = \frac{R_\rho}{U_m^2/2} \left(-\frac{dP_m}{dX}\right) \tag{13}$$

Where P_m and U_m are the dimensionless mean pressure and dimensionless mean velocity, respectively, given by:

$$P_m = \frac{\int_{R_i}^{R_o} PR\,dR}{\int_{R_i}^{R_o} R\,dR} \quad \text{and} \quad U_m = \frac{\int_{R_i}^{R_o} UR\,dR}{\int_{R_i}^{R_o} R\,dR}$$

The average friction factor is obtained by the integration of the local value over the heat exchanger length:

$$f_m = \frac{1}{L}\int_0^L f_x\,dX \tag{14}$$

- *Thermal parameters.* To assess the effect of the porous fins on heat transfer, the local Nusselt number along the outer wall of the inner cylinder is evaluated as:

$$Nu_x = \frac{hD_h}{k_c} = -\frac{\{\lambda(R_k - 1) + 1\}\frac{\partial\theta}{\partial R}\big|_{R=R_i}}{\theta_w - \theta_m} \tag{15}$$

Where h is the convective heat transfer coefficient given by:

$$h = \begin{cases} -\dfrac{k_e\frac{\partial T}{\partial r}\big|_{r=r_i}}{T_w - T_m} & \text{porous regions} \\ -\dfrac{k_c\frac{\partial T}{\partial r}\big|_{r=r_i}}{T_w - T_m} & \text{fluid regions} \end{cases}$$

and θ_m the dimensionless bulk temperature taken as:

$$\theta_m = \frac{\int_{R_i}^{R_o} |U|\theta R\,dR}{\int_{R_i}^{R_o} |U| R\,dR}$$

The average Nusselt number is calculated as follow:

$$Nu_m = \frac{1}{L}\int_0^L Nu_x\,dX \tag{16}$$

The average Nusselt number ratio is defined as:

$$R_{Nu\,m} = \frac{Nu_m}{Nu_{mf}} \tag{17}$$

Where Nu_{mf} is the average Nusselt number in the fluid case.

The heat transfer performance ratio is defined as the ratio of increase in heat transfer to the unit increase in pumping power as done by Ko and Anand (2003) and Miranda and Anand (2004). In this ratio, the pumping power is proportional to $f^{1/3}.Re$, so:

$$\eta = \frac{Nu_m/Nu_{mf}}{(f_m/f_{mf})^{1/3}} \tag{18}$$

The heat exchanger effectiveness defined as the ratio of the actual rate of heat transfer in the heat exchanger (Q_a) to the maximum possible heat transfer rate (Q_{max}) is calculated as:

$$E = \frac{Q_a}{Q_{max}} = \frac{(\dot{m}C_p)_c(\theta_{oc} - \theta_{ic})}{C_{min}(\theta_{ih} - \theta_{ic})} = \frac{(\dot{m}C_p)_h(\theta_{ih} - \theta_{oh})}{C_{min}(\theta_{ih} - \theta_{ic})} \quad (19)$$

Where $C_{min} = \min\left[(\dot{m}C_p)_c, (\dot{m}C_p)_h\right]$, and θ_{oc} and θ_{oh} are the dimensionless temperatures of the cold and hot fluids at the heat exchanger exit.

Numerical procedure

The differential equations (1)-(7) subjected to the boundary conditions given by equations (8)-(12) are solved numerically using the finite volume method. A staggered grid was considered such that the velocity components are located at the control volume faces whereas pressure and temperature are located at the centers of the control volumes. The inertia terms in equations (2) and (3) are linearized as suggested by Patankar (1980). The SIMPLE algorithm is adopted to solve the flow field and the power law scheme is used in the discretizing procedure. The obtained system of algebraic equations is then solved using a line by line technique, combining between the tridiagonal matrix algorithm and the Gauss-Seidel method.

A uniform zonal grid with different step sizes in each region (porous and fluid) is used. The finer meshes are set on both the interfacial regions of the porous fins and near the solid wall regions. To analyze the effect of the grid size on the numerical solution, seven grid systems from 30 × 200 to 200 × 500 (in r and x directions, respectively) are tested as shown in Table I. It is found that the relative error in the average friction factor between the solutions of 150 × 500 and 200 × 500 is 1.2 per cent and in average Nusselt number is 0.8 per cent. In view of saving computation time a grid system of 150 × 500 is chosen for all computations.

For convergence criteria of the iterative process, the relative variations of velocity components and temperature between two successive iterations and the absolute error on the heat flux transferred between the fluids over the entire heat exchanger are required to be smaller than 10^{-5} and 10^{-3}, respectively.

Before proceeding further, it is necessary to ascertain the reliability of the numerical model. To this end, quantitative comparison is made with the results obtained by Bouhadef *et al.* (1999) when a porous layer ($L_f = 0$) is attached to the external wall of the inner cylinder. Figures 2 and 3 show acceptable matching between the two results with an error less than 3 per cent.

Table I.
Grid sensitivity analysis ($L_f = 0.5$, $H_p = 0.8$, $Da = 10^{-6}$ and $R_k = 100$)

Grid number ($r \times x$)	30 × 200	40 × 300	60 × 400	100 × 400	150 × 400	150 × 500	200 × 500
f_m	0.329	0.432	0.344	0.378	0.401	0.413	0.418
Relative error (per cent)	–	31.3	20.4	9.9	6.1	2.9	1.2
Nu_m	8.58	10.89	11.25	11.62	12.06	11.87	11.96
Relative error (per cent)	–	26.9	3.3	3.3	3.8	1.6	0.8

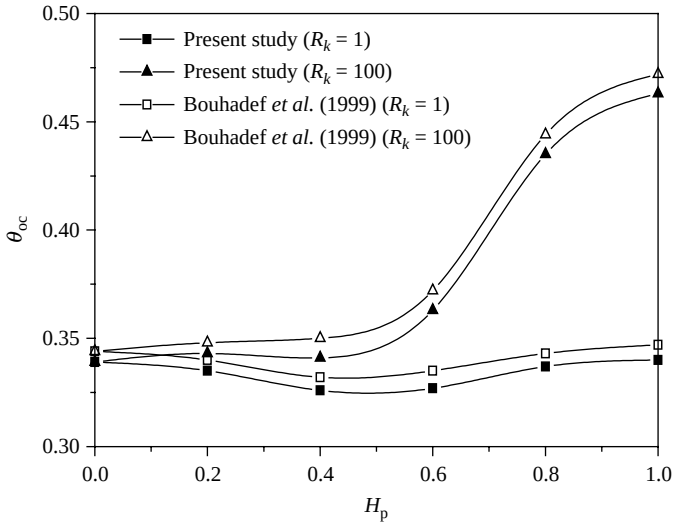

Figure 2.
Outlet temperature of the cold fluid as function of H_p and R_k: $Re = 100$, $Pr = 4$, $L = 50$ and $Da = 10^{-2}$

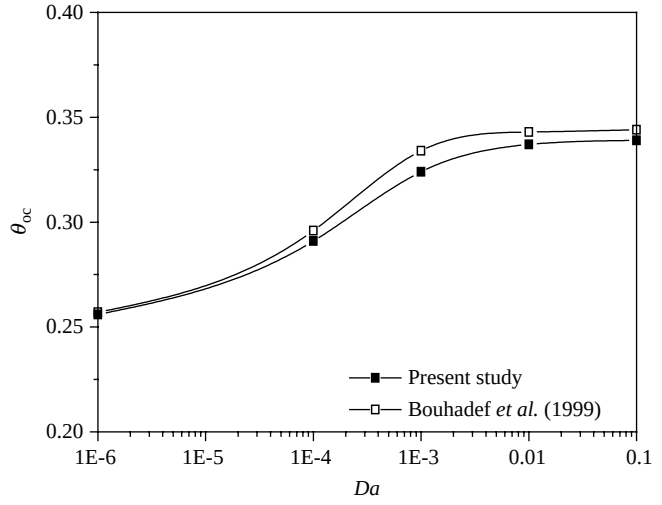

Figure 3.
Outlet temperature of the cold fluid as function of *Da*: $Re = 100$, $Pr = 4$, $L = 50$ and $H_p = 0.8$

Results and discussion

In the present study, the numerical calculations are performed for the fixed input parameters: the radius ratio, the heat exchanger length, the dimensionless length L_a and the porous fins width L_p are set equal to 2, 60, 40 and 0.5, respectively. The value of L_p is chosen such that the size of a fin is larger than that of an elementary representative volume. The flow rates are the same in both ducts ($R_m = 1$), and the same fluid is flowing in the two directions ($R_\rho = 1$, $R_\alpha = 1$, $R_{\mu ch} = 1$, $R_{kch} = 1$). The Prandtl number *Pr* is set fixed at 7 to model water as the working fluid. Since, the value of the effective viscosity in the Brinkman's extension remains controversial, it is taken to be the same as the fluid viscosity, as a first approximation, as done by a lot

of researchers. The porosity and the Reynolds number are set fixed at 0.95 and 300, respectively, and the inertia coefficient CF is taken equal to 0.35 as in the works of Chikh *et al.* (1995a, b, 1997) and Bouhadef *et al.* (1999).

Emphasis here is placed on the effects of Darcy number ($10^{-6} \leq Da \leq 10^{-1}$), the porous fins height ($0 \leq H_p \leq 1$) and spacing ($0 \leq L_f \leq 39$), and the thermal conductivity ratio ($1 \leq R_k \leq 100$) on the hydrodynamic and thermal fields in the annular gap of the heat exchanger.

Hydrodynamic field

Figure 4 shows the effect of Darcy number on the streamlines for a spacing $L_f = 3$ and a height $H_p = 0.8$. At high permeability of the porous medium ($Da = 10^{-2}$), the fluid penetrates into the fins and flows through them easily leading to streamlines slightly distorted. At smaller Darcy number ($Da = 10^{-4}$), the resistance to the flow in the porous regions increases. The fluid rate penetrating the fins is lower than the previous case and therefore the distortion of the streamlines is larger. When $Da = 10^{-6}$, the porous fins tend to be non permeable and behave as solid ones and the fluid escapes to the free space created between the porous medium and the external cylinder. The pressure drop within the fins becomes important so that the fluid above the fins is at a higher pressure than the fluid between them. This makes it flow down and occupy the spacing between the fins yielding the apparition of recirculation zones. These vortices appear downstream to the fins and occupies half of the space between two successive fins. This flow structure will brings an important increase of heat transfer between the wall and the fluid as it will be seen later in the analysis of the thermal field.

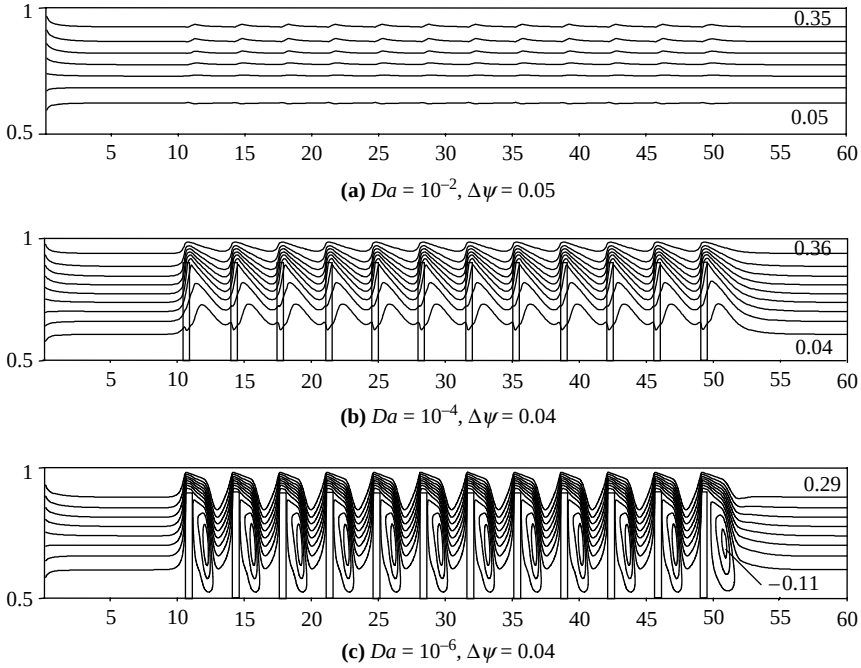

Figure 4.
Effects of the Darcy number on streamlines for $L_f = 3$ and $H_p = 0.8$

The flow pattern is also affected by the porous fins height as it appears in Figure 5. Increasing the height of the fins, when Da is kept at a constant value ($Da = 10^{-5}$), leads to a disruption of the flow and the formation of a vortex behind each fin. When the porous fins occupy the entire annular gap ($H_p = 1$), one observes that the flow is now slightly disrupted and the fluid moves in a fairly uniform fashion.

The effect of the spacing on streamlines for $Da = 10^{-6}$ and $H_p = 0.8$ is shown in Figure 6. At small spacing ($L_f = 0.5$), one notices that a great quantity of the fluid flows in the free space with the formation of recirculation zones occupying all the space between fins which obstruct the flow in the core from coming into contact with the wall. The size of these vortices increases with the augmentation of the spacing (Figure 6(b)). When $L_f = 3$, these vortices are pushed towards the downstream face of each fin and occupy now half of the fins spacing; the fluid coming from the top flowing in the other half in a wavy trajectory which will lead to an augmentation of the heat transfer rate between the cold fluid and the wall. At higher spacing ($L_f = 9$), a region of uniform flow appears between the fins with a slightly smaller vortex behind each of them. This flow structure will lead to lower heat transfer enhancement as it will appear in the analysis of the thermal field.

Thermal field

We will study now the effect of using porous fins on the thermal field structure by analyzing the evolutions of the average Nusselt number and the efficiency of the heat exchanger.

The effect of the fins spacing on Nu_m for various Darcy numbers and a height $H_p = 0.6$ is shown in Figure 7(a). First, it can be observed that at high permeabilities

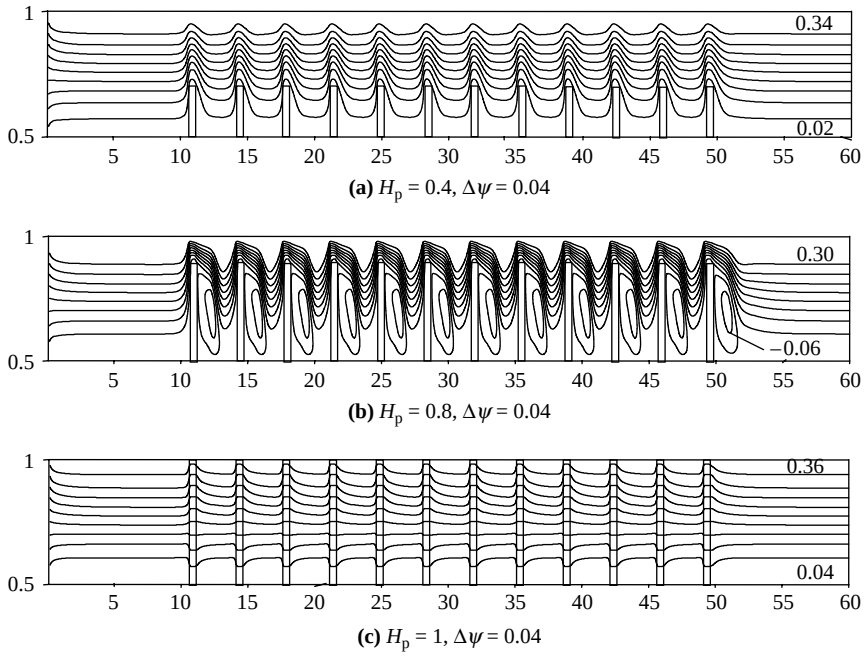

Figure 5.
Effects of the porous fins height on streamlines for $L_f = 3$ and $Da = 10^{-5}$

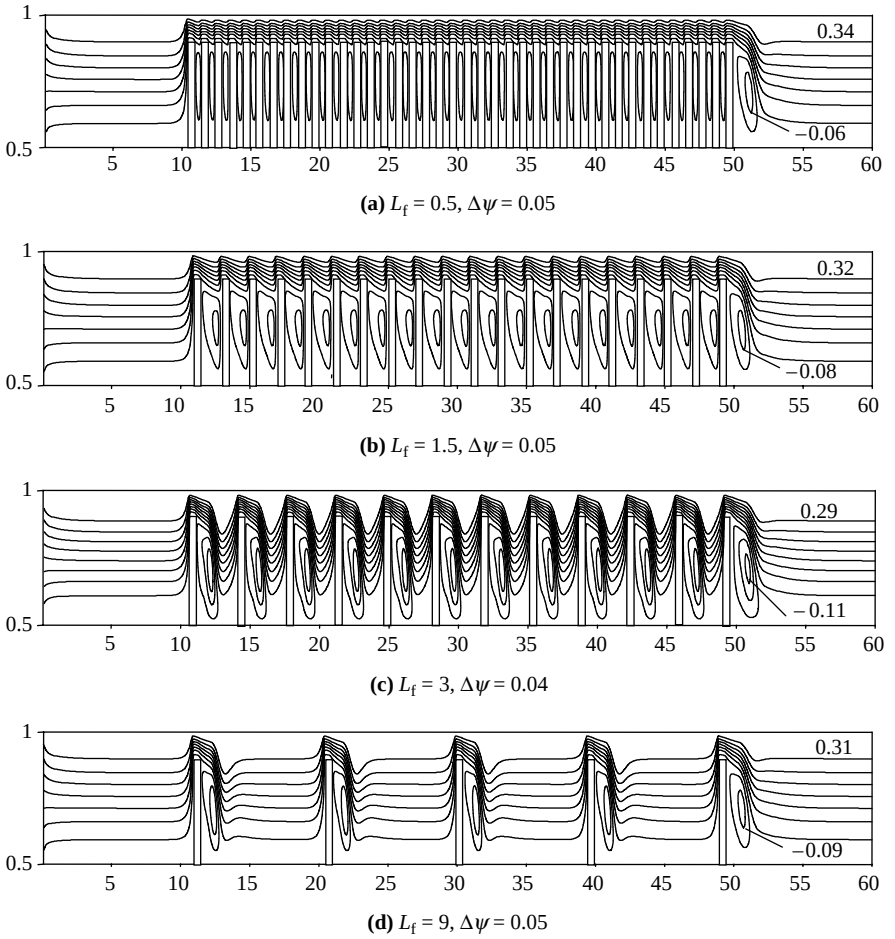

Figure 6.
Effects of the porous fins spacing on streamlines for $H_p = 0.8$ and $Da = 10^{-6}$

($Da \geq 10^{-3}$) the Nusselt number varies slightly with the spacing. This is due to the fact that the increase of the Darcy number leads us more and more towards the case without porous medium and hence the small effect of L_f. At small Darcy numbers ($Da \leq 10^{-4}$), one notices that when the spacing increases the average Nusselt number also increases until it reaches a maximum corresponding to an optimal value of L_f beyond which it decreases and tends towards a constant value. Indeed, since the length on which are attached the porous fins is fixed at $L_a = 40$, the increase of L_f will generate a decrease of the fins number and thus the augmentation of the fluid region with uniform flow. The value of the optimal spacing depends on the permeability; it increases with the decrease of the Darcy number (for instance at $Da = 10^{-4}$, $L_{f\,opt} \approx 0.75$ while at $Da = 10^{-6}$, $L_{f\,opt} \approx 4$).

The variation of the average Nusselt number with the spacing for various porous fins heights and for $Da = 10^{-6}$ is shown in Figure 7(b). One notices that the value of the optimal spacing leading to the highest heat transfer rate depends also on the height;

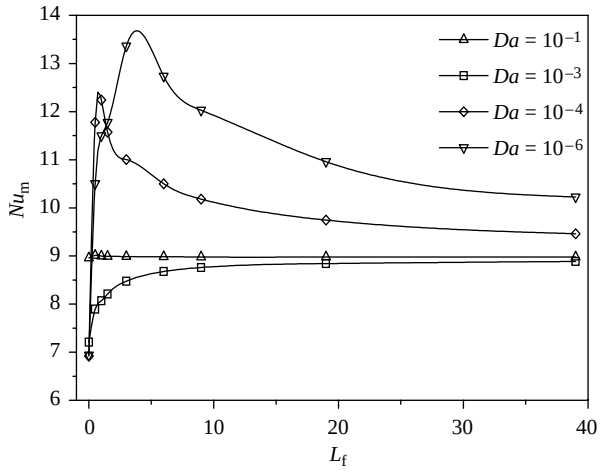

(a) $H_p = 0.6$

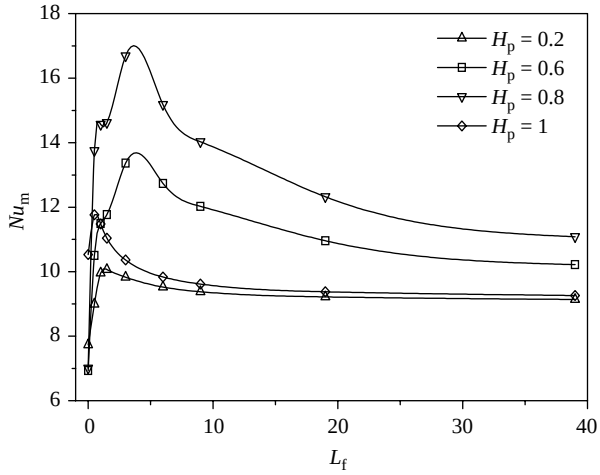

(b) $Da = 10^{-6}$

Figure 7.
Variation of average Nusselt number with porous fins spacing for $R_k = 1$

it increases with fins height (for instance, at $H_p = 0.2$, $L_{f\,opt} \approx 1.25$ while at $H_p = 0.8$, $L_{f\,opt} \approx 3.75$) with, however, its decrease for the case $H_p = 1$ ($L_{f\,opt} \approx 0.6$) due to the weak disturbance of the flow as it was shown in Figure 5(c).

The variation of Nu_m as a function of permeability for a height $H_p = 0.2$ is shown in Figure 8(a). First, it is seen that for all considered spacing, the use of porous fins leads to an improvement of heat transfer in comparison to the porous layer case ($L_f = 0$). Contrary to this latter configuration, where there is an augmentation of the heat transfer rate with the increase of the Darcy number, the configuration in fins gives a better heat transfer with the decrease of the permeability. The evolution of Nu_m with Da also shows the presence of a minimum value of heat transfer rate which occurs at about $Da = 10^{-3}$.

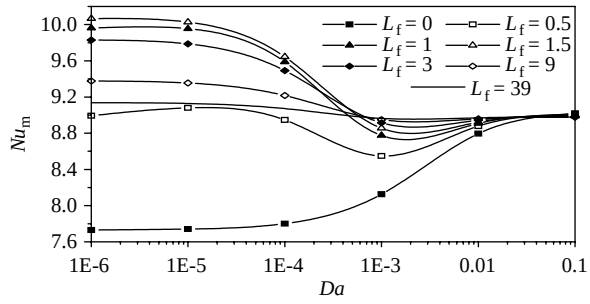

(a) $H_p = 0.2$

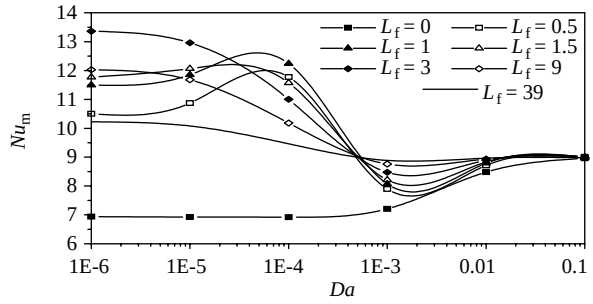

(b) $H_p = 0.4$

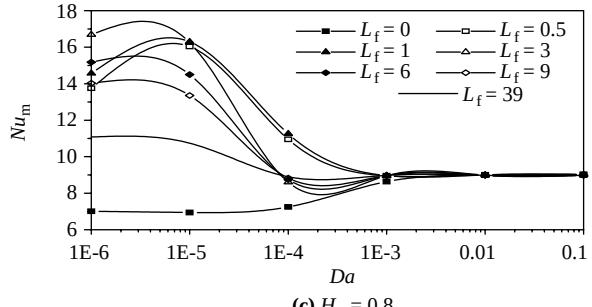

(c) $H_p = 0.8$

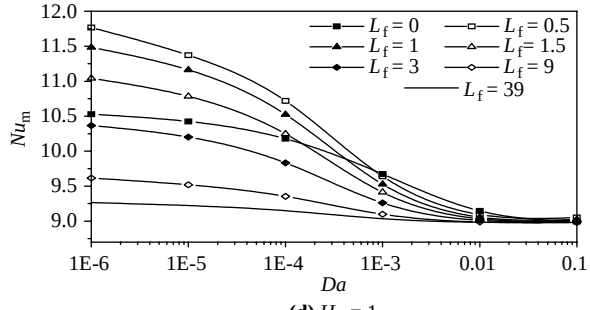

(d) $H_p = 1$

Figure 8.
Variation of average Nusselt number with the Darcy number for $R_k = 1$

Beyond this critical value of permeability, one notices an increase of the average Nusselt number and its tendency at high Da ($Da > 10^{-2}$) towards a constant value corresponding to the fluid case. It is to note that at large spacing ($L_f = 39$, for instance), the Darcy number effect on Nu_m is negligible because of the diminution of the fins number and thus the increase of the fluid region with uniform flow. When $H_p = 0.4$ (Figure 8(b)), it is found that at small spacing ($L_f = 0.5$, 1 and 1.5) the maximum rate of heat transfer is not obtained at $Da = 10^{-6}$ but at higher values of the permeability (between 2×10^{-5} and 5×10^{-5}). At high-fins heights ($H_p = 0.8$, Figure 8(c)) a new behaviour appears: the minimum of heat transfer occurs now at $Da = 10^{-4}$ for spacing $L_f \geq 3$, while the maximum average Nusselt number is obtained for a larger spacing ($L_f = 3$) and for Darcy number close to 10^{-5}. For permeabilities such as $Da \geq 10^{-3}$, Nu_m becomes constant. When the porous fins occupy the entire annular gap ($H_p = 1$, Figure 8(d)), one notices first that the maximum of heat transfer occurs at $Da = 10^{-6}$ for all considered L_f. The comparison between the partially porous case (fins at $H_p = 1$ and $L_f > 0$) and the fully porous case (porous layer at $H_p = 1$ and $L_f = 0$), shows that for $Da \geq 10^{-3}$ the fully porous case is better whatever is the considered spacing while for $Da < 10^{-3}$, it is it only for $L_f > 1.5$.

Figure 9(a) shows the effect of the porous fins height on the average Nusselt number for $Da = 10^{-6}$. It shows an interesting result which is opposite at what is obtained when a porous layer is inserted into the annular gap of the heat exchanger: the rate of heat transfer increases with H_p and this augmentation is not monotonous since there exists an optimal height at which Nu_m reaches its maximum. In this case, the value of this optimal height is $H_p = 0.8$ because of the flow structure which is favourable to the enhancement of heat transfer according to Figures 4(c) and 5(b). Beyond this optimal height, the heat transfer rate decreases but it remains higher than the fluid case. This decrease may be mainly attributed to the fact that the fluid mostly flows between the porous fins and the pipe wall for $H_p \leq 0.8$. Further increase in fins height decreases the clear fluid gap and flow experience high resistance, where the fluid does not have preference region to flow, therefore, the Nusselt number decreases. When the Darcy number increases ($Da = 10^{-4}$, Figure 9(b)), the value of the optimal height is now included between 0.5 and 0.6 according to the spacing. One also observes a minimum of heat transfer at a height $H_p = 0.8$ for spacing $L_f \geq 1.5$. For $Da = 10^{-3}$ (Figure 9(c)), the problem is different due to moderate permeability of the porous medium. A similar evolution to that found in the case of a porous layer is obtained but with an enhancement of the heat transfer by use of fins. When the height increases, the Nusselt number decreases until it reaches a minimum corresponding to a critical height beyond which Nu_m becomes increasing exceeding even the value of the fluid case when $H_p > 0.8$. Similar results were obtained by Bouhadef *et al.* (1999) and Allouache and Chikh (2006) in the case of a porous layer inserted in the heat exchanger.

The results presented previously (Figures 7-9) are for the case of a low-conducting porous fins ($R_k = 1$). Attention is now turned to the discussion of the thermal conductivity ratio effect on the heat exchange between the hot and cold fluids.

Figure 10(a) shown the evolution of the heat exchanger effectiveness with R_k for a spacing $L_f = 3$, various Darcy number and a fins height $H_p = 0.4$. It is shown an increase of E with this ratio because of the increase of the heat transfer rate by conduction towards the fluid. This improvement is more important at high permeabilities ($Da \geq 10^{-3}$) because of the great quantity of the fluid penetrating the

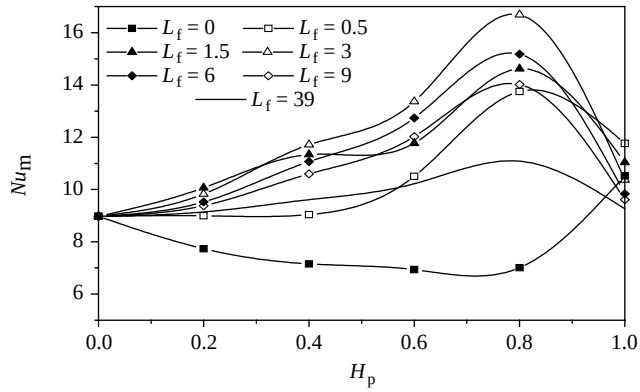

(a) $Da = 10^{-6}$

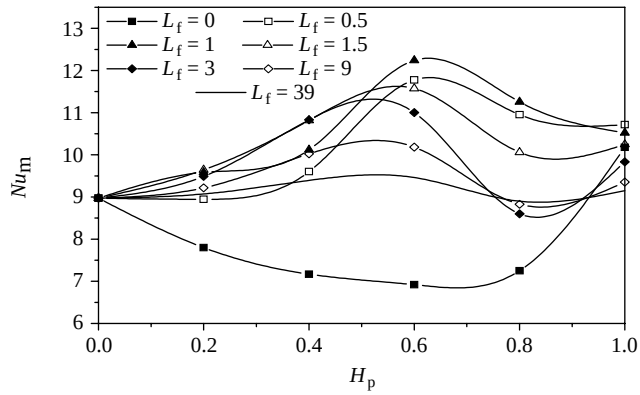

(b) $Da = 10^{-4}$

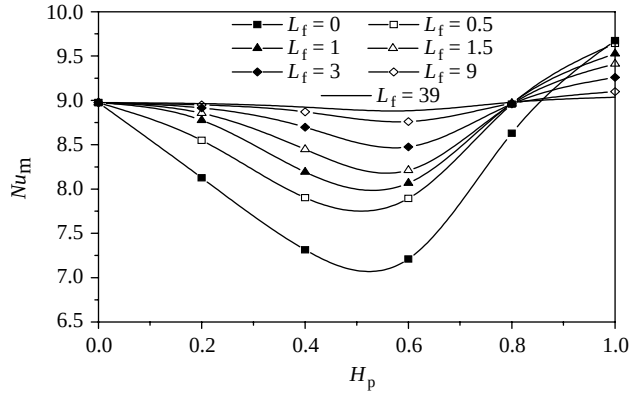

(c) $Da = 10^{-3}$

Figure 9.
Variation of average Nusselt number with the porous fins height for $R_k = 1$

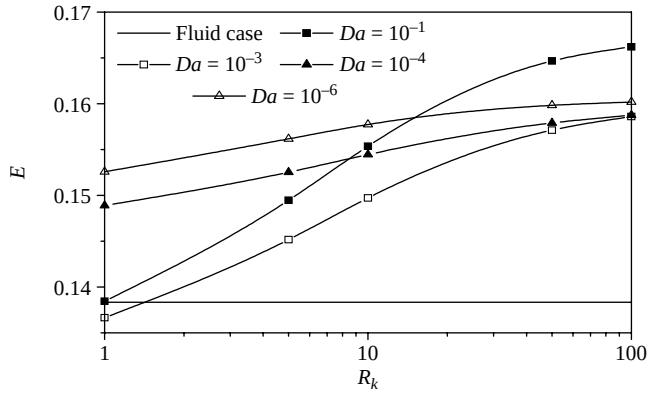

(a) $H_p = 0.4$

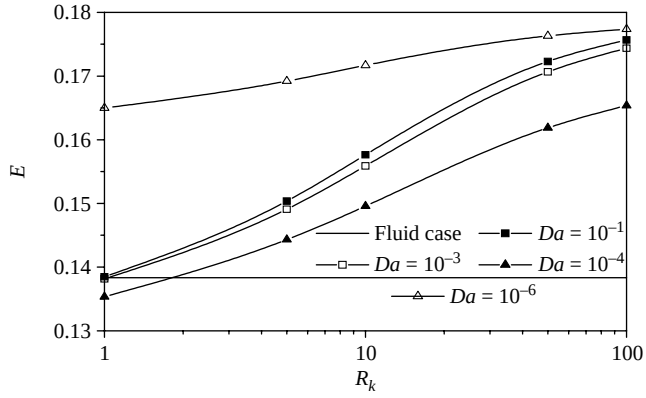

(b) $H_p = 0.8$

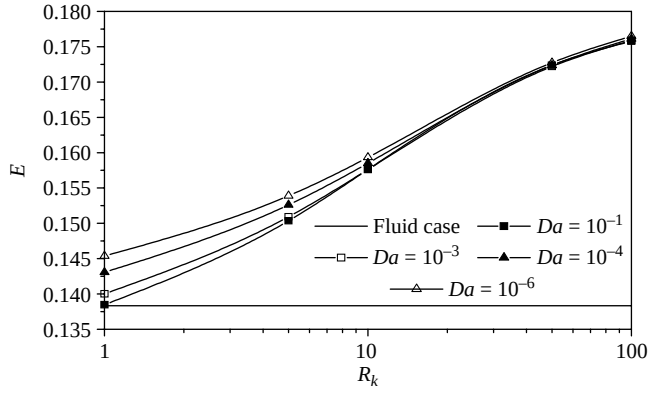

(c) $H_p = 1$

Figure 10.
Heat exchanger effectiveness versus thermal conductivity ratio for $L_f = 3$

porous medium and therefore, a significant extraction of heat at the wall. Beyond a given value of the thermal conductivity, which varies with the permeability ($R_k \approx 8.5$ for $Da = 10^{-4}$ and $R_k \approx 1.5$ for $Da = 10^{-6}$), the case at high permeability becomes the most interesting for enhancing the heat exchanger effectiveness. When the porous fins height increases ($H_p = 0.8$, Figure 10(b)), one notices that the evolution of E with R_k remains unchanged with a higher increase of the effectiveness at high-Darcy numbers ($Da \geq 10^{-3}$) and the case $Da \leq 10^{-5}$ leading always to the highest effectiveness and it will probably be necessary to increase the thermal conductivity ratio beyond the value of 100 so that the fins at high permeabilities become more effective than those at small Darcy numbers. When the fins occupy the entire annular gap ($H_p = 1$, Figure 10(c)), it is seen that from $R_k \approx 20$ the permeability has a weak effect on the value of E.

This behaviour of the heat exchanger effectiveness with R_k was found in the case of a porous layer configuration in the works of Bouhadef *et al.* (1999), Alkam and Al-Nimr (1999) and Allouache and Chikh (2006).

Regarding the variation of the average Nusselt number with the thermal conductivity ratio it appears, according to Figure 11, a similar behaviour to that obtained for the effectiveness. Such a result was also found by Miranda and Anand (2004) in the case of porous baffles mounted in a rectangular channel.

Thermal performance

We will try now to evaluate the effectiveness of using the arrangement of the porous medium in fins. The porous layer configuration is also presented for comparison.

The first parameter which we considered is the ratio of the average Nusselt number in the porous fins case to the average Nusselt number in the fluid case and which we noted $R_{Nu\,m}$.

In Figure 12, the evolution of this ratio with the Darcy number by varying the fins spacing and the height and by fixing the thermal conductivity ratio to unity is shown. First, one notices that the heat transfer is improved by use of fins in comparison to the case of a porous layer which gives, for $Da < 10^{-1}$ and $H_p < 1$, a $R_{Nu\,m}$ lower than unity indicating that the porous medium can be used in that case as an insulator. For these same conditions the porous fins are more efficient than the fluid case and lead to an average Nusselt number ratio greater or equal to unity for permeabilities such as $Da < 10^{-3}$. The highest values of this ratio are obtained at small Darcy numbers and at high heights ($(R_{Nu\,m})_{max} \approx 1.95$ is obtained at $H_p = 0.8$, $Da \approx 3.5 \times 10^{-6}$ and $L_f = 3$). When $H_p = 1$, this ratio is greater than unity whatever are the values of the Darcy number and spacing. In this case, the arrangement in porous layer becomes attractive and even better than the arrangement in fins at small Darcy numbers ($Da < 10^{-3}$) for spacing greater than 1.5 and at high permeabilities ($Da \geq 10^{-3}$) whatever is the value of L_f.

There are various performance evaluation criteria, however, it is difficult to decide on the proper one for heat transfer enhancement because numerous factors enter into the ultimate decision as pumping power or operating cost, maintenance cost (cleaning), safety, reliability ... However, it is possible to choose some performance criteria for preliminary design guidance. It is what was made in the present work where the second parameter studied to evaluate the effectiveness of using porous fins is the heat transfer performance ratio η. It is defined in the same manner as in the works of Ko and Anand (2003) and Miranda and Anand (2004): it is the ratio of heat transfer enhancement to unit increase in pumping power. As every improvement technique

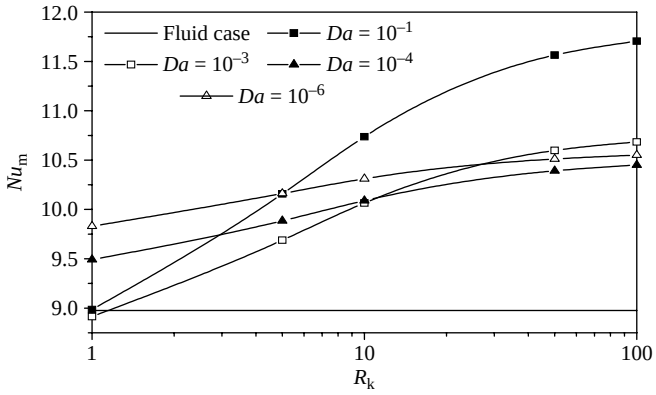

(a) $H_p = 0.2$

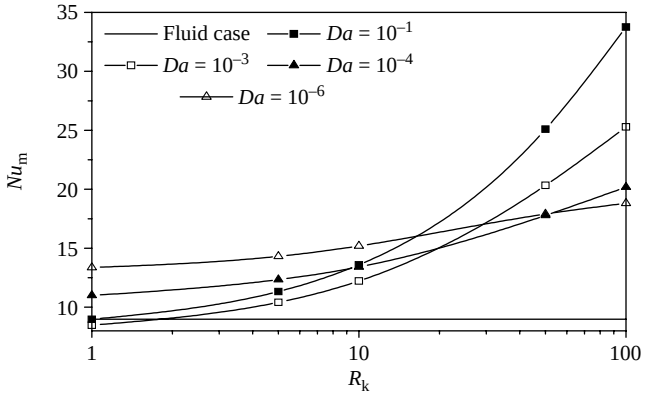

(b) $H_p = 0.6$

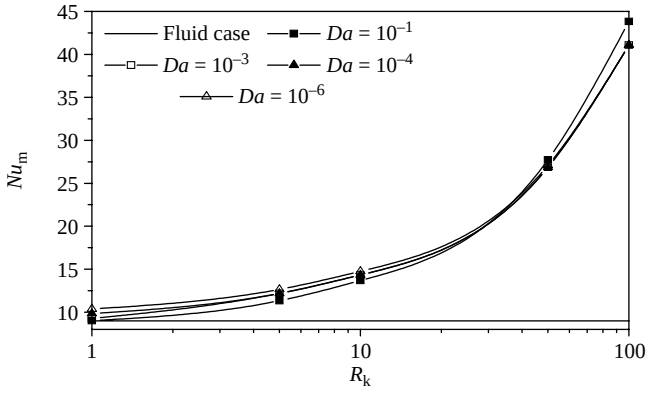

(c) $H_p = 1$

Figure 11.
Average Nusselt number versus thermal conductivity ratio for $L_f = 3$

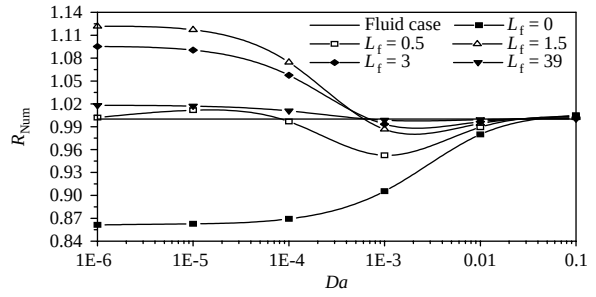

(a) $H_p = 0.2$

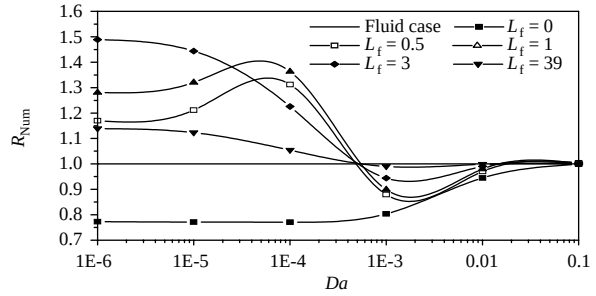

(b) $H_p = 0.6$

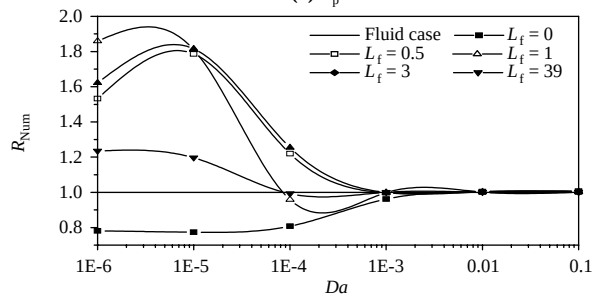

(c) $H_p = 0.8$

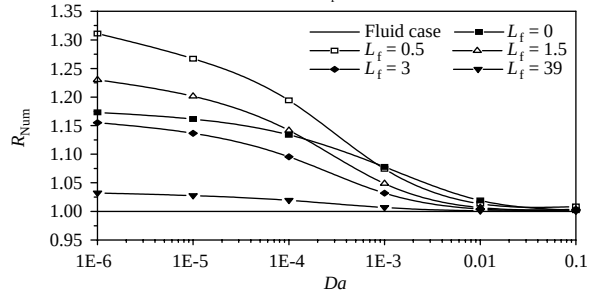

(d) $H_p = 1$

Figure 12.
Average Nusselt number ratio as function of *Da* for different H_p and $R_k = 1$

introduces pressure drop which could be important, this ratio can represent the net energy gain or net energy loss which can be achieved. Thus, if the used technique is attractive, this parameter will have to be greater than unity. The evolution of η with the Darcy number for various spacing and heights of the porous medium and for $R_k = 1$ is shown in Figure 13. First, it is observed that the porous layer leads to the smallest heat transfer performance ratio for all the considered cases (η is always lower than unity). This means that the use of a porous layer will causes energy loss rather than a gain. At small heights of the porous fins ($H_p = 0.2$, Figure 13(a)), the friction being not very important, this arrangement leads to values of the heat transfer performance ratio greater than unity for Darcy numbers lower than 10^{-4} and for fins spacing $L_f > 0.5$. In this case, $\eta_{max} \approx 1.06$ is obtained at $Da = 10^{-6}$ and at $L_f = 1.5$. By increasing the fins height ($H_p = 0.4$, Figure 13(b)), the value of this ratio slightly increased ($\eta_{max} \approx 1.1$ is obtained at $Da = 10^{-6}$ and at $L_f = 3$) but it is higher than unity only for spacing greater than 1.5. As the friction is very important at $H_p = 0.8$ and $H_p = 1$ than the heat transfer enhancement, the values of η obtained in these cases are always lower than unity (Figure 13(c) and (d)) in spite of the case $H_p = 0.8$ is generally the one which gave the highest average Nusselt numbers.

We also examined the effect of the thermal conductivity ratio on the value of η. The results for $R_k = 100$ are shown in Figure 14. One notices for this case of highly conducting material that the arrangement in porous fins becomes interesting since η is significantly increased, especially at high permeabilities and heights, due to heat transfer improvement further to the increase of the thermal conductivity ratio. For this value of R_k the arrangement in porous layer leads to the highest values of the performance ratio for $Da > 10^{-4}$ when $H_p < 1$ and whatever is the value of the permeability when $H_p = 1$. An interesting practical case springs of this figure corresponding to a permeability such as $Da = 10^{-3}$. Indeed, in this case the arrangement in porous fins can be considered as an attractive technique for improving the performances of a heat exchanger since it leads to high values of the performance ratio, which are always greater than the unity ($\eta_{max} \approx 8$ at $H_p = 1$ and $L_f = 0.5$) with moderate pressure drops in comparison to the solid fins.

Conclusion

The current study is a numerical modelling of fluid flow and heat transfer in a double pipe heat exchanger with porous fins inserted in the annular gap. The effects of several geometrical, physical and thermal parameters such as fins spacing and height, Darcy number and the thermal conductivity ratio on the structure of the hydrodynamic and thermal fields are analyzed. The main results obtained can be summarized in the following:

(1) At small permeabilities and high heights of the porous fins, the flow is strongly disrupted and there is appearance of circulation zones of size depending on the spacing between two successive fins.

(2) There is an optimal value of the fins spacing leading to the highest heat transfer rate. Its value depends on the permeability and on the height.

(3) For a thermal conductivity ratio $R_k = 1$, the highest average Nusselt number is obtained at small permeabilities and at high heights.

(4) The porous layer for heights $H_p < 1$, yields for all the considered cases a smaller heat transfer rate than the fins. When $H_p = 1$, these latter structures are more efficient than the fully porous case only at small spacing and Darcy numbers.

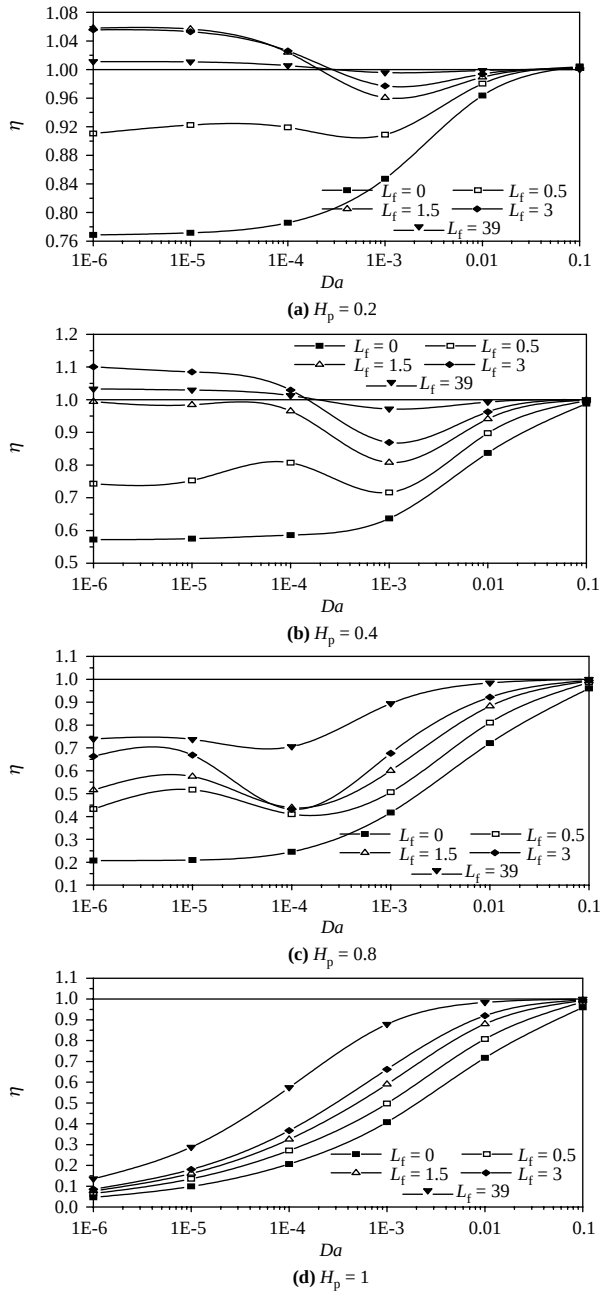

Figure 13.
Heat transfer performance ratio as function of *Da* for different H_p and $R_k = 1$

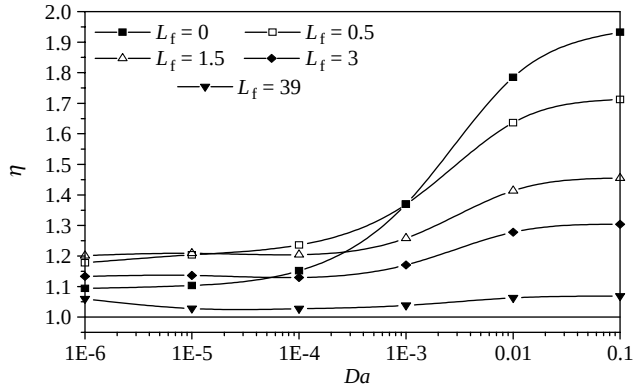

(a) $H_p = 0.2$

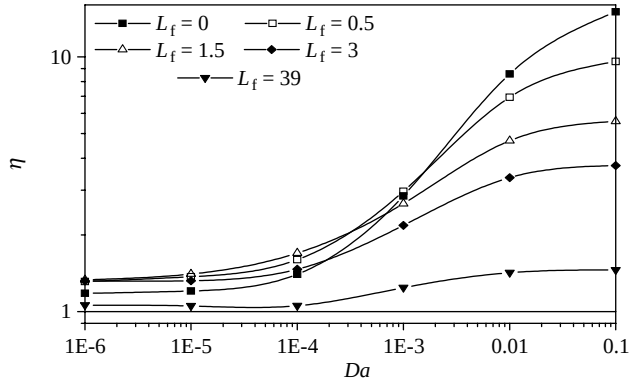

(b) $H_p = 0.6$

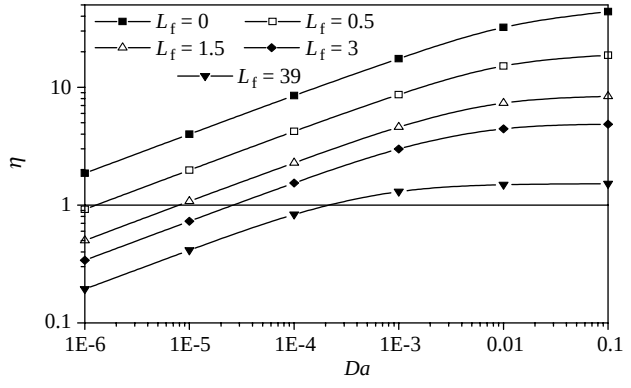

(c) $H_p = 1$

Figure 14.
Heat transfer performance ratio as function of *Da* for different H_p and $R_k = 100$

(5) The increase of the thermal conductivity ratio is interesting especially at high permeabilities and heights of the porous fins.

(6) The study of the average Nusselt number ratio revealed that the arrangement in fins at $R_k = 1$ leads to an important improvement of the heat transfer, in comparison to the fluid case, at high heights and small permeabilities. For the present study, we have obtained $(\mathrm{R}_{Nu\,\mathrm{m}})_{\max} \approx 1.95$ at $H_\mathrm{p} = 0.8$, $Da \approx 3.5 \times 10^{-6}$ and $L_\mathrm{f} = 3$.

(7) The introduction of the heat transfer performance ratio η, allowed finding optimal values of Da, H_p and L_f for which the use of porous fins becomes an attractive technique (in that case $\eta > 1$):

- The highest performance ratio obtained in this study, at $R_k = 1$, was found for $L_\mathrm{f} = 3$, $H_\mathrm{p} = 0.4$ and $Da = 10^{-6}$ ($\eta_{\max} = 1.1$).
- By increasing the thermal conductivity ratio ($R_k = 100$), the values of η are significantly increased and the arrangement in porous fins becomes more efficient especially at high permeabilities and heights. Thus, it is recommended that for an effective heat transfer enhancement, the use of porous fins with higher permeability (for example, $Da = 10^{-3}$) and thermal conductivity must be opted for (gain in fins material and pumping cost in comparison to solid fins).

References

Alkam, M. and Al-Nimr, M.A. (1999), "Improving the performance of double-pipe heat exchangers by using porous substrates", *International Journal of Heat and Mass Transfer*, Vol. 42, pp. 3609-18.

Allouache, N. and Chikh, S. (2006), "Second law analysis in a partially porous double pipe heat exchanger", *Transactions of the ASME Journal of Applied Mechanics*, Vol. 73, pp. 60-5.

Bouhadef, K., Chikh, S., Boumedien, A. and Lauriat, G. (1999), "Effect of porous substrate addition on heat exchanger efficiency", IMechE Transactions C565/021/99, pp. 13-18.

Chikh, S., Boumedien, A., Bouhadef, K. and Lauriat, G. (1995a), "Analytical solution of non-Darcian forced convection in an annular duct partially filled with a porous medium", *International Journal of Heat and Mass Transfer*, Vol. 38 No. 9, pp. 1543-51.

Chikh, S., Boumedien, A., Bouhadef, K. and Lauriat, G. (1995b), "Non-Darcian forced convection in an annulus partially filled with a porous material", *Numerical Heat Transfer, Part A*, Vol. 28, pp. 707-22.

Chikh, S., Boumedien, A., Bouhadef, K. and Lauriat, G. (1997), "Amélioration du transfert thermique par un dépôt poreux sur la paroi d'un échangeur tubulaire", *Revue Gnénérale de Thermique*, Vol. 36, pp. 41-50.

Guo, Z., Sung, H.J. and Hyun, J.M. (1997), "Pulsating flow and heat transfer in an annulus partially filled with porous media", *Numerical Heat Transfer, Part A*, Vol. 31, pp. 517-27.

Kiwan, S. and Al-Nimr, M.A. (2001), "Using porous fins for heat transfer enhancement", *Transactions of the ASME Journal of Heat Transfer*, Vol. 123, pp. 790-5.

Ko, K.H. and Anand, N.K. (2003), "Use of porous baffles to enhance heat transfer in a rectangular channel", *International Journal of Heat and Mass Transfer*, Vol. 46, pp. 4191-9.

Miranda, B.M.D.S. and Anand, N.K. (2004), "Convective heat transfer in a channel with porous baffles", *Numerical Heat Transfer, Part A*, Vol. 46, pp. 425-52.

Patankar, S.V. (1980), *Numerical Heat Transfer and Fluid Flow*, McGraw-Hill, New York, NY.

Pavel, B.I. and Mohamad, A.A. (2004), "An experimental and numerical study on heat transfer enhancement for gas heat exchangers fitted with porous media", *International Journal of Heat and Mass Transfer*, Vol. 47, pp. 4939-52.

Yang, Y.T. and Hwang, C.Z. (2003), "Calculation of turbulent flow and heat transfer in a porous baffled channel", *International Journal of Heat and Mass Transfer*, Vol. 46, pp. 771-80.

About the authors

H. Kahalerras received the degree in Hydraulic Engineering, ENP, Algiers; Master and PhD in Mechanical Engineering from Grenoble University, France in 1993, 1994 and 1997, respectively. During 1997-2000, Kahalerras worked as a Head Assistant and from 2000 to 2001 as a Lecturer in USTHB, FGMGP, Algiers. Since 2001, Kahalerras has been working as a Head Lecturer in USTHB, FGMGP, Algiers. The courses which are taught by Kahalerras are: strength of materials, fluid mechanics, heat transfer and fluid flow in porous media. H. Kahalerras is the corresponding author and can be contacted at: kahalerrashenda@yahoo.fr

N. Targui received the degree in Mechanical Engineering and Master in Mechanical Engineering in USTHB, Algiers in 1998, 2006, respectively. Since 2006, Targui has been working as a Head Assistant in University of Blida, Algeria. The courses taught by Targui are: industrial drawing and electricity.